Investigating the electric properties of a siliciclastic reservoir based on rock-physics modeling and laboratory experiments

Zhong Wang

Dissertation for Ph.D. degree

Faculty of Mathematics and Natural Sciences
Department of Geosciences
University of Oslo
Norway

September 2009

Series of dissertations submitted to the
Faculty of Mathematics and Natural Sciences, University of Oslo
Nr. 882

ISSN 1501-7710

Cover: Inger Sandved Anfinsen.
Printed in Norway: AiT e-dit AS, Oslo, 2009.

Produced in co-operation with Unipub AS.
The thesis is produced by Unipub AS merely in connection with the
thesis defence. Kindly direct all inquiries regarding the thesis to the copyright
holder or the unit which grants the doctorate.

Unipub AS is owned by
The University Foundation for Student Life (SiO)

Preface

This thesis is submitted for the Philosophy Doctor degree in Petroleum Geophysics at the Section of Petroleum Geology and Geophysics (PEGG), Department of Geosciences, University of Oslo. This study has been financially supported by the Research Council of Norway (NFR) and StatoilHydro within the framework of PETROMAKS (Programme for the Optimal Management of Petroleum Resources) through the project 'Honoring the complexity of the petroleum reservoir- a new modeling tool for sea bed logging'. One of the main goals of the project has been to extend Controlled-Source EM (CSEM) forward modeling by including a proper electric rock-physics description of a hydrocarbon reservoir. An extensive conductivity model of reservoir rocks based on Differential Effective Medium (DEM) theory has been developed. It was integrated with both 1.5D and 2.5D CSEM forward modeling tools and the potential of this combined method to describe possible production effects of the CSEM response was demonstrated. A parallel work has been to modify a triaxial cell so that it can carry out simultaneous resistivity and acoustic measurements at reservoir conditions. A variety of such tests employing core samples have been carried out to calibrate rock-physics models and to gain basic understanding of the electric and elastic properties of reservoir rocks.

The outcomes of this study are briefly presented in an introduction giving the background, main objectives and contributions made followed by three scientific papers (two published and one submitted) and four proceeding papers. The first paper focuses on the development of the DEM model and the second and third papers discuss the modification of the triaxial cell and the corresponding simultaneous resistivity and acoustic measurements on core samples. The first three proceeding papers discuss implementations of various rock-physics models within CSEM forward modeling tools and show the influence of rock properties on the CSEM response. The last proceeding paper compares the efficiency of different antenna types and orientations for detecting hydrocarbon layers employing CSEM.

Acknowledgements

This work has been carried out at both the Department of Geosciences, University of Oslo (UiO) and at the Norwegian Geotechnical Institute (NGI). Funding was provided by the Norwegian Research Council (NFR) and StatoilHydro through the project 'Honoring the complexity of the petroleum reservoir- a new modeling tool for sea bed logging'.

This thesis would not have been accomplished without the help of several persons. My foremost thanks go to my supervisors Prof. Leiv-J. Gelius at UiO and Dr. Fan-Nian Kong at NGI for introducing me to this subject. Their patience and encouragement have helped me to face the challenges I met during my research. I am grateful to Prof. Leiv-J. Gelius, my principal supervisor, for active guidance on thrashing out challenges regarding theories and experiments of rock physics and countless hours devoted to revision of all my papers and this thesis. I would like to thank Dr. Fan-Nian Kong, my co-supervisor, for numerous help on my work on theories and modeling of electromagnetics.

I wish to thank NGI for providing me with work place and experimental facility to complete my thesis. My colleagues at NGI's Department of Instrumentation and Geophysics are most appreciated in their support and friendship.

My special thanks go to Toralv Berre, Gudmund Havstad, Sven Vangbæk, Erik Lied, Reidar Otter and Trude Ørbech for their tremendous support during the experimental work at NGI. I appreciate the support of Berit L. Berg and Turid Winje at the Department of Geosciences, University of Oslo for XRD and SEM analyses.

I would particularly thank Ivar Brevik and Anne-Kari Furre at StatoilHydro for their inspiration and interest in my work.

I thank my wife Yun Mou who always encouraged me, and provided support of emotion and daily life during those years. I appreciate her understanding with my long working hours at the laboratory. Lastly, I thank my parents for their understanding and support on my career.

Contents

List of publications

Paper 1: Gelius, L.-J and Wang, Z., 2008. Modelling production caused changes in conductivity for a siliciclastic reservoir: a differential effective medium approach, Geophysical Prospecting, **56**, 677-691.

Paper 2: Wang, Z., Gelius, L.-J. and Kong, F.N., 2009, Simultaneous core sample measurements of elastic properties and resistivity at reservoir conditions employing a modified triaxial cell – a feasibility study, Geophysical prospecting , published online , doi: 10.1111/j.1365-2478.2009.00792.x.

Paper 3: Wang, Z. and Gelius, L.-J., 2009. Electric and elastic properties of rock samples – a unified measurement approach (submitted to Petroleum Geosciences)

PIERS extended abstract (1): Wang, Z. and Gelius, L.-J., 2007. Modeling of Seabed Logging Data for a Sand-shale Reservoir. Progress in Electromagnetic Research Online, Vol 3, No 2, 236-240.

EAGE extended abstract: Wang, Z., Gelius, L.-J. and Kong, F.N., 2007. Influence of Temperature on the Seabed Logging Response of a Sand-shale Reservoir, 69th EAGE Conference, London, Extended Abstract D044.

SEG extended abstract: Wang, Z., Gelius, L.-J. and Kong, F.N., 2008. A sensitivity analysis of the sea bed logging technique with respect to reservoir heterogeneities, SEG Annual Meeting 2008, Las Vegas, 711-715.

PIERS extended abstract (2): Johnstad, S.E., Westerdahl, H. Kong, F.N. and Wang, Z, 2007. Comparison of Antenna Types and Orientations for Detecting Hydrocarbon Layers in Seabed Logging. Progress in Electromagnetic Research Online, Vol 3, No 1, 52-55.

1. Introducton

Marine Controlled-Source EM (CSEM)

During the later years the use of the controlled-source electromagnetic (CSEM) method (or seabed logging) within hydrocarbon exploration has evolved rapidly (Eidesmo et al. 2002; Srnka et al. 2006; Constable and Srnka 2007; Darnet et al. 2007). Although seismic is still the far more important and effective method for imaging potential reservoir zones, its combined use with electromagnetic data increases significantly the sensitivity to discriminate between pore fluid. Fig. 1 shows the schematic principle of the CSEM technique. A horizontal electrical dipole towed by a vessel is employed as transmitter antenna emitting electromagnetic energy. A receiver array is deployed along the sea floor receiving the electromagnetic signals from all directions. If a resistive hydrocarbon-bearing reservoir exists, the guided wave in the reservoir has less attenuation and thus the received signal by receivers will be larger than the case without a hydrocarbon-bearing reservoir. The potential of discriminating oil and brine bearing reservoirs makes the CSEM technique a useful complement to the seismic method traditionally employed in the oil and gas industry.

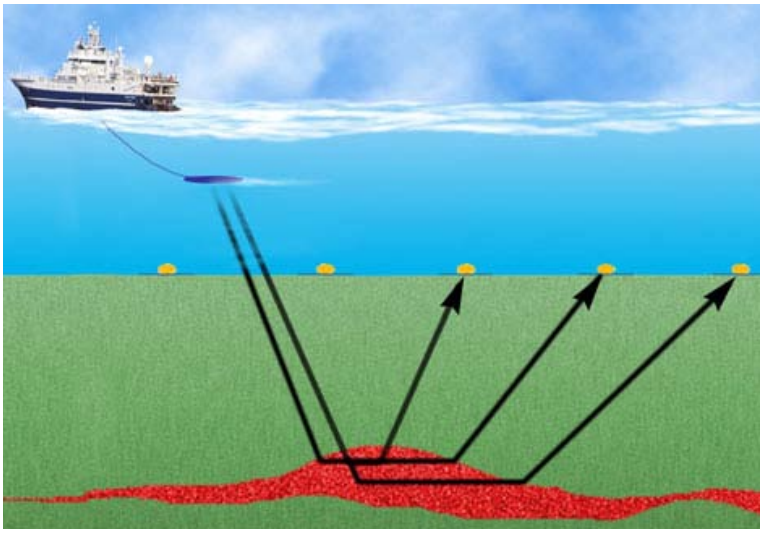

Fig. 1 Vessel tows a high-power electromagnetic source while recording the direct, reflected, and refracted signals on the seabed. (Source: Statoil)

However, marine CSEM is still a relatviely new technique and many ambiguities related to the concept need to be further investigated. The further success of the technique relies on an improved understanding of the electric earth model combined with the development of optimized and cost-effective exploration procedures. Up till now the link between modeled data employed in CSEM and the actual electromagnetic description of the medium has been rather crude. This work proposes an alternative to standard CSEM forward modeling by integrating it with an electric rock-physics formulation. Such a combined approach makes it feasible to investigate production caused effects due to variations in temperature, stress and

saturations. In addition, making use of log information and rock-physics can possibly improve CSEM inversion and thus derive the corresponding reservoir characteristics. The joint interpretation of CSEM, logging data and rock-physics can be employed to monitor hydrocarbon saturation changes in producing reservoirs (by analogy with 4-D seismic). Therefore, the link between CSEM and rock- physics is of major interest.

Rock physics

To address the problem of computing the conductivity (alternatively the resistivity) of porous reservoir rocks, various mixing models have been introduced during the year. The simplest version of such theories only give bounds (Wiener 1912; Madden 1976; Halliday,Resnick and Walker 1997; Hashin and Shtrikman 1962; Milton and Kohn 1988). More advanced effective-medium theories like the Maxwell-Garnet equation (Maxwell-Garnet 1904; Wagner1914; Bergman 1978) assume different spherical inclusions embedded in a conducting host medium. These inclusions do not interact, hence implying a dilute assumption. In the Bruggeman model (Bruggeman 1935; Landauer 1952), which is also called the self-consistent effective medium approximation, each type of inclusion is in interaction with the (effective) medium. These two types of models have traditionally received criticism of their accuracy since the dilute model ignores the inclusion interaction while the self-consistent model overestimates it. A further refinement is represented by the differential effective medium theory, where the host phase percolates for the full range of fractions and the second phase (inclusions) may or may not conduct. In the embedding scheme, the inclusions are added to the host material in infinitesimal amounts, which leads to the so-called Hanai-Bruggeman equation (Bruggeman 1935; Hanai 1960a, b). At the limit of nonconducting dispersed particles, the Hanai-Bruggeman equation simplifies to Archie's law (Archie 1942). This law is frequently employed in petrophysics to analyze resistivity logs. For non-clean sands, more generalized versions of Archie's law exist. The simplest modification includes simple empirical correction factors (Carothers 1968; Porter and Carothers 1970), whereas the Waxman-Smits model (Waxman and Smits 1968) addresses the problem of shaly sand in a more systematic manner. The original Waxman-Smits model is valid for a fully water-saturated rock and it was later extended to the partially-saturated case by Waxman and Thomas (1974), who also discuss the effect of temperature.

In the literature, the differential effective medium schemes for computing the effective conductivity of reservoir rock mostly fall into one of two categories: two-phase or three-phase material.

In the case of two-phase materials, the differential effective medium model represents a mixture of conducting rock grains and water, describing the case of shaly sandstone where clay occurs as a grain coating. Mendelson and Cohen (1982) discuss this approach in detail and also consider the effect of randomly-oriented grains as well as aligned elliptical grains. Bussian (1983) employed the same type of model but also allowed for complex conductivities. Revil et al. (1998) combined Bussian's model with an explicit description of the behavior of ions in the pore space, employing so-called Hittorf transport numbers. Lima and Sharma (1990) alternatively described the coated-clay case by an idealized spherical geometry, which implies that the conductivity of the coated grains can be computed from the lower Hashin-Shtrikman bound (1962). Lima et al. (2005) discuss the two-phase differential effective medium equation further by considering the freshwater shaly sandstone case and also make a comparison to the general mixing theory. Niwas, Gupta and de Lima (2006) discuss asymptotic approximations of the two-phase differential effective medium scheme.

In the case of three-phase material, Lima and Sharma (1990) discuss a mixture of water, insulating spherical sand grains and spherical clay inclusions. This model aims to describe the dispersed clay case, where clay is distributed in the pore volume.

All the differential effective medium schemes discussed above have in common that they are derived for a fully water saturated case. They are not therefore directly applicable to porous rocks saturated with different fluids. To partly compensate for this, hybrid formulations involving additional empirical mixing laws, like the hydrocarbon first principle (Lima and Sharma 1990) are introduced. Rabaute, Revil and Brosse (2003) also used a differential effective medium approach for clay-coated sandstones, combined with mixing laws for both saturated and unsaturated conditions. However, Feng and Sen (1984) employed a three-phase differential effective medium model to describe a partially water-saturated case (e.g., a mixture of brine and hydrocarbons) but their formulation is only valid for clean sand. In shaly sandstones, clay can also be distributed both as coated clay and dispersed in the pore volume (Lima and Sharma 1990), however, none of the existing differential effective medium schemes can handle the combined case of insulating sand grains and conducting inclusions being either dispersed or coated clay.

These observations have motivated the development of the differential effective medium formulation in this study. This extended scheme can handle the partially saturated case involving a mixture of both water and hydrocarbons for shaly sandstone. Moreover, it allows for both coated and dispersed clay, including a possible alignment for the latter case. Various sand grain distributions including grain alignment (anisotropy) are also allowed for. Of equal importance is that the new differential effective medium scheme is also conditioned for the reservoir production (monitoring) application, which implies that the effect of changes in temperature, stress, salinity and saturation are all integrated as part of the formulation.

To support the development of rock-physics models and also to gain basic understanding of the electric behavior of reservoir rocks, development of laboratory equipment to measure the electric (as well as the elastic) properties of core samples at reservoir condition can be very useful. Hence, the development of a modified triaxial cell has been an integrated part of this study. Moreover, combined elastic and electric data can also be employed to constrain joint inversion of seismic, CSEM and log data with the potential of giving an improved reservoir description.

Simultaneous resistivity and acoustic measurements employing a modified triaxial cell

Triaxial cells are commonly used in rock mechanic tests. Traditionally they can measure strain, deformation, and the elastic velocities of rock samples at complex conditions. The stress and temperature conditions of the cell can be controlled, and the external load as well as the fluid imbibitions and drainage can be varied during tests. Within the oil and gas industry, triaxial cells are usually used to measure elastic properties (i.e., P- and S- wave velocities, bulk and shear moduli, etc.). Recently due to the introduction of the CSEM technique, the interest in measuring the resistivity of reservoir rock samples has increased rapidly. However, in most cases, the elastic properties and the resistivity are measured separately in the laboratory employing different transducers and sample holders. It is therefore difficult to keep exactly the same experimental conditions (i.e. temperature, stress and saturation and avoid

velocity-stress hysteresis) if tests are run separately. This motivated the development of a modified triaxial cell tailored for joint electric/elastic measurements at complex conditions.

A modification was introduced to an existing triaxial cell by using the top cap and the pedestal as electrodes to measure the axial resistivity of rock samples. Fig. 2 shows the schematic drawing of the modified triaxial cell. In the original cell acoustic transducers were already mounted at the top cap and the pedestal (Berre, 1981; Chryssanthakis et al., 1999).

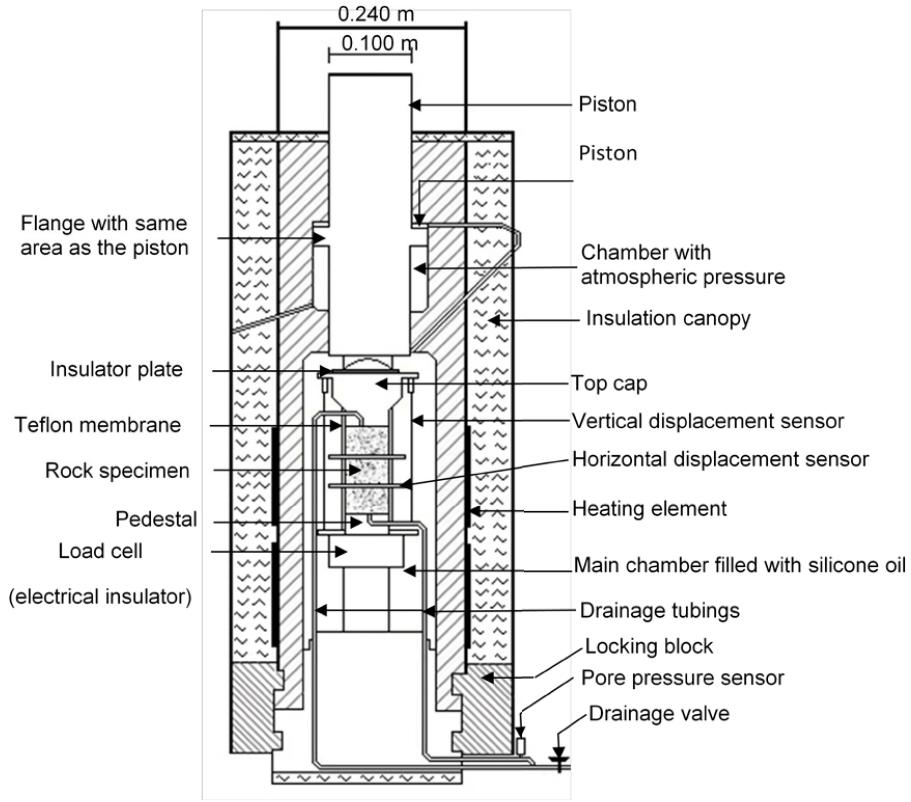

Fig. 2 Schematic drawing of the modified triaxial cell that can measure conventional acoustic parameters as well as resistivity at reservoir conditions. The P- and S- wave transducers are encapsulated in the top cap and pedestal, which also serve as electrode for resistivity measurements.

Since a two electrode system has been used in the modified triaxial cell, the electrode polarization effect will distort the resistivity measurements at low frequencies when the sample is saturated with brine (Janz and Ives, 1968; McAdams et al., 1995; Lapatki et al., 2003).

Systematic studies have been carried out to minimize the electrode polarization impedance within the modified triaxial cell. Simulations and calibrations show that the electrode polarization impedance can be minimized by employing a proper selected frequency band and

source magnitude as well as electrode material (i.e., coating the steel electrodes by a thin layer of copper).

In addition, a strap electrode system has been developed for measuring the radial resistivity of a cylindrical specimen. The relationship between the measured resistance and the actual resistivity of the samples can be calculated numerically. Radial resistivity measurements can be employed to investigate possible electrical anisotropy of the rock samples. In addition, it represents an alternative choice to measure resistivity of a rock sample when axial resistivity is not available.

Employing the modified triaxial cell as a platform, a series of simultaneous core sample measurements of resistivity and elastic properties have been carried out. The influence of temperature and pressure on both the resistivity and the elastic properties of various rock samples have been investigated. Correlations between conductivity, elastic properties (e.g. P- and S- wave velocities, bulk and shear moduli), porosity and permeability have been established theoretically and tested against laboratory measurements. Electrical anisotropy has also been estimated and analyzed employing a X-ray image analysis. In addition, simultaneous monitoring of both resistivity and acoustic velocity has been demonstrated during a water substituting oil process.

Employing the modified triaxial cell, various rock-physics models have been compared with laboratory measurements including the differential effective medium model developed in this study.

Combination of rock-physics and CSEM

Employing the DEM resistivity model, the effective conductivity of a hydrocarbon reservoir can be estimated based on the knowledge of its rock-physics properties (e.g. porosity and oil/gas saturation). The effective conductivity can be interfaced to a CSEM forward modeling tool, thus the reservoir properties can be linked to the CSEM response.

In this study, a 1.5D CSEM forward modeling software/tool has been developed based on the theory developed by Kong (1972). The source can be a horizontal electric dipole (HED), a vertical electric dipole (VED), a horizontal magnetic dipole (HMD) or a vertical magnetic dipole (VMD). The geological structure is assumed to be 1D, but the electrical anisotropy of the stratified model has been taken into account. Source and receivers can be deployed at arbitrary positions within the stratified geological structure. In addition, the software also has a graphic user interface (GUI). Employing this 1.5D model, the sensitivity of choosing different antenna types and orientations for detecting hydrocarbon layers in CSEM, has been investigated.

Another software package, which is able to calculate the effective conductivity of reservoir rocks based on various rock-physics models, has also been developed and can be interfaced to the CSEM forward modeling tool. The rock-physics simulator includes bound models, self-consistent models, diluted models, empirical models, and the DEM models developed in this study. It also has a graphic user interface (GUI).

Employing the rock-physics simulator and the 1.5D CSEM modeling tool, the rock-physics properties of a reservoir can be linked to the CSEM response. In addition, a 2.5D CSEM modeling tool based on the finite element method (FEM) (Kong et al., 2008) was also

employed. This 2D formulation can represent more complex reservoirs and makes the combination with the rock-physics simulator more flexible and realistic.

By including knowledge of rock-physics, forward modeling tools can be better employed to carry out feasibility studies in connection with hydrocarbon detection. In addition, future use of the CSEM technique is foreseen to be within reservoir monitoring during production, employing permanent multi-component/multi-wave receiver arrays on the seafloor. In order to carefully monitor the differences in the electromagnetic response from such a production reservoir over time, rock-physics models help to understand the resistivity changes caused by variations in saturations, pressure and temperature. The CSEM inversion can also be improved by integration with rock-physics and logging data and thus the hydrocarbon reservoir can be characterized (e.g. estimate of total gas volume).

The combined modeling approach obtained by interfacing standard CSEM forward modeling programs (1.5D or 2.5D) with a rock-physics simulator has been employed in this study to investigate:

- The influence of various clay types and their distribution in a shaly reservoir.
- The influence of temperature in case of steam injection (secondary EOR).
- The influence of lithological heterogeneities (i.e., porosity and stress).
- The influence of saturation changes in connection with water flooding (imbibition process).

2. Objectives of this study

The aim of this study has been to integrate the use of rock-physics within the CSEM technique. The specific objectives of the research can be stated as:

- Development of a rock-physics model for a proper electrical description of a hydrocarbon reservoir during production. This model should handle partial saturations involving a mixture of both water and hydrocarbons and take into account different types of clay and their distribution. Possible variations in shape and alignment (anisotropy) for both sand grains and clay aggregates should also be included. Since this rock-physics model is to be used to predict production effects, variations in temperature, stress, salinity and saturation should all be allowed for.
- Development of a measurement system making it feasible to measure simultaneously the elastic and electric properties of core samples at complex (reservoir) conditions. Employing this system, the validity of both electric and elastic rock-physics models can be investigated and correspondingly calibrated. The electrical properties of reservoir core samples (e.g. anisotropy, frequency dependency, contribution from clay and formation water, the influence of temperature and stress, etc.) should be investigated. The simultaneous resistivity and elastic measurements should be used to investigate the correlations between different rock properties (e.g. resistivity, elastic properties, porosity, permeability, etc.). In addition, the measurement system should

also be employed to monitor both resistivity and elastic properties during a production process (e.g. water flooding oil).

- Integrating rock-physics within CSEM modeling by interfacing a rock-physics simulator with standard EM forward modeling tools. Therefore, a combined software system needs to be developed and implemented. It should then be employed to study how various production caused effects will modify the CSEM response.

To achieve these objectives, a DEM rock-physics model has been developed describing changes in resistivity for a siliciclastic reservoir under production. This formulation represents modification and extensions made to previous work tailored for well logging purposes. The validity of the DEM model has been tested against previously published rock-physics models as well as laboratory measurements. Further, a triaxial cell has been modified to make simultaneous measurements of both electric and elastic properties feasible. This modified cell has been systematically calibrated and a variety of tests have been carried out to establish correlations between different rock properties. In addition, a 1.5D CSEM forward modeling tool and a software package including various rock-physics models have been developed. By combining these two tools, a more proper link between the rock-physics properties and the CSEM response has been established.

3. Main scientific contributions

The section gives an overview of the three scientific papers and the four proceeding papers presented in this study. The first paper focuses on the development of the DEM model and the second and third papers discuss the modification of the triaxial cell and the simultaneous resistivity and acoustic measurements on core samples. The first three proceeding papers discuss implementations of various rock-physics models within CSEM forward modeling tools and demonstrate the influence of rock properties on the CSEM response. The last proceeding paper compares the efficiency of different antenna types and orientations for detecting hydrocarbon layers employing CSEM.

Paper 1

In this paper, a rock-physics model based on differential effective medium (DEM) theory has been developed. It can be used to predict resistivity changes associated with a reservoir during production. The DEM model has been calibrated employing both published and own laboratory measurements. In addition, the DEM model has been interfaced to a CSEM forward modeling tool. The influences on the CSEM response caused by variations in salinity, water saturation, temperature and pressure have been simulated. The main contributions and conclusions of this paper can be summarized as follows:

- The DEM model represents further extensions and modifications of previous works developed for well logging. It can handle the partially saturated case as well as account for possible variations in both shape and alignment (anisotropy) of both sand grains and clay. In addition, the DEM model can also be employed for reservoir monitoring purposes since the effects of changes in temperature and pressure have been integrated as part of the formulation.

- The validity of the DEM model has been investigated employing both published as well as own laboratory measurements. In general, the rock-physics model fits these data well for both clean and shaly reservoir rock samples.

- The DEM model has been linked to a 1D EM modeling program. Correspondingly, the effects on the CSEM response of varying salinity, water saturation, temperature and stress have been simulated. These simulations show that the salinity, water saturation and temperature significantly influence the reservoir resistivity whereas the stress is much less important.

Paper 2

In this paper, a triaxial cell has been modified to accomplish simultaneous resistivity and acoustic measurements at complex (reservoir) conditions. The modified triaxial cell has been systematically calibrated and a series of tests have been carried out. These measurement data were used to calibrate various rock physics models. The main contributions and conclusions in this paper can be summarized as follows:

- A triaxial cell, which was originally designed for acoustic measurements, has been modified to include resistivity measurements as well. The two-electrode system used for axial resistivity measurements was calibrated systematically.

- The electrode polarization effect caused by the contact between electrodes and salt water in the two-electrode system can be minimized by taking several measures, i.e., employing a proper frequency band and source magnitude as well as a proper choice of electrode material (i.e., by coating the steel electrodes by a thin layer of copper).

- The influence of stress on both resistivity and elastic properties has been investigated. The tests show that stress changes affect elastic properties (e.g. P- and S- wave velocities, bulk and shear moduli, etc.) significantly whereas it has less impact on the resistivity. In addition, the resistivity changes observed during a varying stress experiment can be estimated from the measurements of the elastic properties employing porosity as a bridge.

- The influence of temperature on both resistivity and elastic properties has also been investigated. The tests show that temperature changes have a significant effect on the resistivity whereas less on the elastic properties. This supports the future use of CSEM within reservoir monitoring during a steam-injection process.

- In addition, the influence of water saturation on both resistivity and P- wave velocity has been investigated. The tests show that the resistivity is much more sensitive than the P- wave velocity to changes in the water saturation. This indicates that CSEM is better than seismic to trace hydrocarbons when the oil/gas saturation is low (e.g. 30%).

- To complement the axial resistivity measurement, a strap-on radial electrode system has been developed and calibrated. Electrical anisotropy was observed by measuring both axial and radial resistivities on a brine-saturated rock sample.

Paper 3

This paper discusses a series of experiments carried out employing the modified triaxial cell introduced in paper 2. The aim is to obtain further understanding about both the electrical and elastic properties of reservoir rocks. In addition, correlations between different rock properties have been systematically investigated employing both rock-physics models as well as laboratory measurements. The main contributions and conclusions in this paper can be summarized as follows:

- Six core samples from three different wells (and characterized employing XRD and SEM analyses) were employed to investigate possible correlations between conductivity, P- and S- wave velocities, porosity and permeability. Identified experimental trends were then tested against a variety of rock-physics models. A good correlation was obtained in most cases.

- The effect of formation water on the EM response was investigated. It was found that except at very high ions concentrations, the resistivity was rather insensitive to different salt solutions.

- Electrical anisotropy of a brine-saturated rock sample was investigated by measuring both axial and radial resistivity. Anisotropy was observed and this finding was supported by X- ray images obtained from a CT scanner.

- A water substituting oil process carried out at reservoir condition was monitored by using frequency-dependent resistivity measurements. This study indicated that the electrical properties are much more sensitive than elastic properties in case of water flooding associated with enhanced oil recovery. The magnitude and phase of the complex resistivity were measured and frequency dispersion was observed at different oil saturations. In general, the magnitude of the resistivity decreased significantly with increasing water saturation, whereas the corresponding phase seemed rather insensitive to the saturations.

PIERS extended abstract (1)

This paper represents the first attempt to demonstrate the feasibility of interfacing rock-physics modeling with standard EM modeling. A 1-D forward modeling code developed in this study was interfaced with a sample of previously published EM rock-physics models taken from well logging. The study investigates how the CSEM response is being influenced by variations in salinity and also by introducing different types of clay distributions. The simulations show that a high salinity corresponds to a large effective conductivity of the reservoir rock and consequently a low EM detectability. Moreover, it is shown that different clay distributions in a hydrocarbon reservoir will cause different effective conductivities with structural clay showing the highest effective conductivity and the laminated clay showing the lowest one. Correspondingly, a laminated clay reservoir will have the largest CSEM response.

EAGE extended abstract

The work presented here can be considered as a direct continuation of the study given in the PIERS extended abstract (1). This time the influence of temperature on the conductivity of both brine and clay has been investigated. Again the 1-D forward modeling code was

interfaced to an existing rock-physics model (i.e., the work by Sen and Goode, 1992). The variation of the CSEM response caused by temperature changes during a production process was then simulated. Simulations show that temperature plays an important role regarding the effective resistivity of the reservoir. It is therefore of vital important to take into account the influence of temperature on the CSEM response during a temperature varying monitoring experiments.

SEG extended abstract

This paper represents the most complete demonstration of the combined modeling approach. A 2.5D EM modeling code was now interfaced to the comprehensive DEM rock-physics formulation derived in Paper 1. For a 2D reservoir structure, the effects on the final CSEM response caused by lateral variations in lithological parameters like porosity and shaliness was investigated. In both cases the simulations indicated that the sensitivity of possible lateral gradients was poor when compared with the homogeneous average-value case. Hence, reservoir heterogeneities caused by lateral variations in lithology are not picked up easily by the CSEM technique due to its low-frequency limitation. However, in the second set of simulations the cause of the heterogeneities were due to variations in saturations in connection with a producing reservoir. Both the effects of secondary recovery represented by water flooding as well as steam injection were simulated. The potential of the CSEM technique for such monitoring purposes was clearly demonstrated.

PIERS extended abstract (2)

In this paper, the effect of employing different antenna types and orientations for detecting hydrocarbon layers was analyzed. Simulations show that only three types of sources: VED, HED (in-line) and HMD (cross-line) are sensitive to the target – a thin horizontal hydrocarbon layer. The other types of sources: VMD, HED (cross-line), HMD (in-line) are not sensitive to the hydrocarbon layer.

4. Conclusions

Considering the complete study, the main contributions and conclusions can be summarized as follows:

- A rock-physics model based on differential effective medium (DEM) theory for electrical description of a hydrocarbon reservoir has been developed. The DEM model can handle partial saturations involving a mixture of both water and hydrocarbons and takes into account variations in shape and alignment (anisotropy) of both sand grains and clay aggregates. In addition, the DEM model can also be employed to predict production caused changes in the resistivity since the effect of changes in temperature, stress, salinity and saturation are all integrated as part of the formulation.

- A modified triaxial cell has been developed that can measure simultaneously both electric and elastic properties at complex (reservoir) conditions. Employing this equipment the validity of both electric and elastic rock-physics models were tested and calibrated employing experimental measurements. In addition the feasibility of using the simultaneous measurement principle has been demonstrated for a large series of different core sample studies.

- The feasibility of the combined modeling approach has been demonstrated in practice, and used to study a series of production caused changes. By combing conventional EM modeling with a rock-physics description a more proper link is established between the actual reservoir properties and the measured CSEM response.

- The present study has been limited to the task of carefully modeling the CSEM response based on a comprehensive rock-physics formulation. Future use of such a combined modeling tool can be as an engine in the inversion of CSEM data or eventually in a joint inversion with seismic. To constrain such inversions, experimental data as those obtained from the modified triaxial cell presented here, can be useful. Also the modified cell makes it feasible to carry out experiments over a broad range of frequencies (10Hz- 5 kHz). Hence, it can be used as a link between the high-frequency logging data and the very low frequency CSEM data. Finally, the combined modeling approach can also be a powerful tool to analyze the sensitivity of the CSEM technique to reservoir parameter changes during production.

5. References

Archie G.E. 1942. The electrical resistivity log as an aid in determining some reservoir characteristics. *Petroleum Technology,* **1**, 55– 62.

Bergman D.J. 1978. The dielectric constant of a composite material – A problem in classical physics. *Physics Reports,* **43**, 377–407.

Berre T. 1981. Triaxial testing at the Norwegian Geotechnical Institute. *Norwegian Geotechnical Institute publication*, No. 34.

Bruggeman D.A.G. 1935. Berechnung verschiedener physikalischer Konstanten von heterogenen Substanzen. *Annalen der Physik,* **24**, 636–679.

Bussian A.E. 1983. Electrical conductance in a porous medium. *Geophysics,* **48**, 1258–1268.

Carothers J.E. 1968. A statistical study of the formation factor relation. *The Log Analyst,* **9**, 13–20.

Chryssanthakis P., Rose E., Westerdahl H., Rhett D. and Pederson S. 1999. High temperature triaxial tests with ultrasonic measurements on Ekofisk chalk, *Rock Mechanics for Industry: Proceedings of the 37th Rock Mechanics Symposium*, 373-379.

Cohen R.W., Cody G.D., Coutts M.D. and Abeles B. 1973. Optical properties of granular silver and gold films. *Physical Review B***, 8**, 3689–3701.

Constable S. and Srnka L.J. 2007. An introduction to marine controlled-source electromagnetic methods for hydrocarbon exploration. *Geophysics* **72**, 2, WA3-WA12.

Darnet M., Choo M.C.K., Plessix R.E., Rosenquist M.L., Cheong K.Y., Sims E. and Voon

J.W.K. 2007. Detecting hydrocarbon reservoirs from CSEM data in complex settings: Application to deepwater Sabah, Malaysia. *Geophysics* **72**, 2, WA97-WA103.

Eidesmo T., Ellingsrud S., MacGregor L.M., Constable S., Sinha M.C., Johansen S., Kong F.N. and Westerdahl H. 2002. Sea Bed Logging (SBL), a new method for remote and direct identification of hydrocarbon filled layers in deepwater areas, *First Break*, **20**, 3, 144-152.

Feng S. and Sen P.N. 1985. Geometrical model of conductive and dielectric properties of partially saturated rocks. *Journal of Applied Physics,* **58**, 3236–3243.

Halliday D., Resnick R. andWalker J. 1997. *Fundamentals of Physics*. John Wiley.

Hanai T. 1960a. Theory of the dielectric dispersion due to the interfacial polarization and its applications to emulsions. *Kolloid- Zeitschrift,* **171**, 23–31.

Hanai T. 1960b. A remark on "Theory of the dielectric dispersion due to the interfacial polarization and its applications to emulsions". *Kolloid-Zeitschrift,* **175**, 61–62.

Hashin Z. and Shtrikman S. 1962. A variational approach to the theory of effective magnetic permeability of multiphase materials. *Journal of Applied Physics,* **33**, 3125–3131.

Janz G.J. and Ives D.J.G. 1968. Silver-silver chloride electrodes. *Ann. N.Y. Acad. Sc.* **148**, 210-221.

Kong, F. N., S. E. Johnstad, T. Røsten and H. Westerdahl, 2008, A 2.5D finite-element-modeling difference method for marine CSEM modeling in stratified anisotropic media: *Geophysics*, **73**, F9-F19.

Kong, J.A., 1972, Electromagnetic fields due to dipole antennas over stratified anisotropic media: *Geophysics*, **37**, 985-996.

Landauer R. 1952. The electrical resistance of binary metallic mixtures. *Journal of Applied Physics,* **23**, 779–784.

Lapatki B.G., Stegeman D.F. and Jonas I.E. 2003. A surface EMG electrode for the simultaneous observation of multiple facial muscles. *Journal of Neuroscience Methods* **123**,117-128.

Lima de O.A.L. and Sharma M.M. 1990. A grain conductivity approach to shaly sandstones. *Geophysics,* **55**, 1347–1356.

Lima de O.A.L., Clenneli M.B., Nery G.G. and Niwas S. 2005. A volumetric approach for the resistivity response of freshwater shaly sandstones. *Geophysics,* **70**, F1–10.

Madden T.R. 1976. Random networks and mixing laws. *Geophysics,* **41**, 1104–1125.

Maxwell-Garnet J.C. 1904. Colours in metal glasses and in metallic films. *Philosophical Transactions of the Royal Society of London,* **203**, 385–420.

McAdams E.T., Lackermeier A., McLaughlin J.A. and Macken D. 1995. the Linear and Non-

linear Electrical Properties of the Electrode-electrolyte Interface. *Biosensors & Bioelectronics* **10**, 67-74.

Milton G.W. and Kohn R.V. 1988. Variational bounds on the effective moduli of anisotropic composites. *Journal of Mechanical Physics of Solids,* **36**, 597–629.

Rabaute A., Revil A. and Brosse E. 2003. *In situ* mineralogy and permeability logs from downhole measurements. Application to a case study in clay-coated sandstone formations. *Journal of Geophysical Research***, 108**, 2414.

Revil A., Cathles L.M., Losh S. and Nunn J.A. 1998. Electrical conductivity in shaly sands with geophysical applications. *Journal of Geophysical Research,* **103**, 23925–23936.

Porter C.R. and Carothers J.E. 1970. Formation factor-porosity relation derived from well log data. SPWLA 11th Annual Logging Symposium Los Angeles, May 3–6.

Sen P.N. and Goode P.A. 1992. Influence of temperature on electrical conductivity on shaly sands. *Geophysics,* **57**, 89–96.

Srnka L., Carazzone J., Ephron M. and Eriksen E. 2006. Remote reservoir resistivity mapping. *The Leading Edge* **25**, 972-975.

Wagner K.W. 1914. Erklarung der Dielektrischen Nachwirkungen auf Grund Maxwellscher Vortellungen. *Arch. Electrotech.* **2**, 371–387.

Waxman M.H. and Smits L.J.M. 1968. Electrical conductivities in oil-bearing shaly sands. *SPE Journal,* **8**, 107–122.

Waxman M.H. and Thomas E.C. 1974a. Electrical conductivities in shaly sands – I. The relation between hydrocarbon saturation and resistivity index. *Journal of Petroleum Technology,* **26**, 213–218.

Waxman M.H. and Thomas E.C. 1974b. Electrical conductivities in shaly sands – II. The temperature coefficient of electrical conductivity. *Journal of Petroleum Technology,* **26**, 218 – 225.

Wiener O. 1912. *Abh. S¨achs. Akad. Wiss. Leipzig Math. Naturwiss.Kl.* **32**, 509.

Paper 1

Modeling production caused changes in conductivity for a siliciclastic reservoir: a differential effective medium approach

By

Gelius, L.-J and **Wang, Z.**

Geophysical Prospecting, 2008

56, 677-691

Paper 2

Simultaneous core sample measurements of elastic properties and resistivity at reservoir conditions employing a modified triaxial cell – a feasibility study

By

Wang, Z., Gelius, L.-J. and Kong, F.N.

Geophysical Prospecting, 2009

Published online, doi: 10.1111/j.1365-2478.2009.00792.x.

Paper 3

Electric and elastic properties of rock samples – a unified measurement approach

By

Wang, Z. and Gelius, L.-J.

Petroleum Geoscience, 2009

(Submitted)

PIERS extended abstract (1):

Modeling of Seabed Logging Data for a Sand-shale Reservoir

By

Wang, Z. and Gelius, L.-J.

Progress in Electromagnetic Research Online, 2007

Vol. 3, No. 2, 236-240

Modeling of Seabed Logging Data for a Sand-shale Reservoir

Zhong Wang and Leiv-J. Gelius
Department of Geosciences, University of Oslo, Norway

Abstract— a new rock-physics modeling tool was developed to describe the electric properties of a sand-shale reservoir. Four types of clay distribution models were implemented to describe possible sand-shale reservoirs including anisotropy. The corresponding algorithms gave as output an estimate of the efficient-medium conductivity of the reservoir. The tool was interfaced to a 1.5-D EM-modeling program used to simulate Seabed logging data. The potential of this integrated modeling approach was demonstrated by calculating the variation in the EM response associated with a petroleum reservoir, due to different clay distributions as well as different brine salinities.

DOI: 10.2529/PIERS060907053724

1. INTRODUCTION

Seabed logging (SBL) is a new method employing EM energy to detect and characterize hydrocarbon bearing reservoirs in marine environments [8]. However, compared with other more mature EM methods, the representation of the target (e.g., the petroleum reservoir) is still rather crude in standard SBL-modeling programs. The reservoir zone is often assigned a fixed conductivity value without any link to a rock physics description. However, the actual petroleum reservoir is a complex mixture of fluid, sand, clay and gas. Different formations and structures will give rise to different EM properties and at the end to different measurements. An accurate and efficient EM description of the reservoir zone is therefore necessary to further understand and develop the SBL technique.

2. ROCK-PHYSICS MODELING

This study is limited to the sand-shale petroleum reservoir. In the sand-shale formation, clay minerals have a substantial effect to the overall equivalent conductivity of the rock. We have implemented four types of mixing-models to describe different clay distributions. In most mixing models one will calculate the effective conductivity of the water and hydrocarbons before calculating the whole rock conductivity. This is the hydrocarbons first method which we also employ here. Assuming zero conductivity of the oil particles, it follows from an Archie type of formula [1]:

$$\sigma_f = \sigma_w S_w^n \tag{1}$$

where σ_f is the effective fluid conductivity, σ_w is the water conductivity and S_w is the water saturation. The factor n is the saturation exponent which is typically between 1.7 and 2. Note that the salinity of the formation water strongly determines its conductivity.

2.1. Mixing-model 1: Structural Clays

In this model the clay grains act as framework grains without altering the reservoir properties. Hence, none of the pore space is occupied by clay. For structural clays we can employ the Bussian/Hanai-Bruggeman equation [2] with low-frequency limit.

$$\sigma^* = \sigma_f \phi^m \left(\frac{1 - \sigma_s/\sigma_f}{1 - \sigma_s/\sigma^*} \right)^m \tag{2}$$

where σ_s is the effective mean volume conductivity of the grains:

$$\sigma_s = p\sigma_c + (1-p)\,\sigma_{sa} \tag{3}$$

and p is the volume fraction of clay in the solid portion, σ_c is the conductivity of the clay and σ_{sa} is the conductivity of the sand (quartz) grains. In Eq. (2) ϕ is the porosity and m is the so called cementation factor assumed to be in the range from 1.7 to 2.3 for a consolidated material. For a clay-rich sand where the water/fluid is such that conduction is dominated by the grains ($\sigma_s \gg \sigma_f$) a simplified version of Eq. (2) can be derived [5].

2.2. Mixing-model 2: Coated Clays

In the *coated-clay* model the clay grains actually coat the sand grains. When clay coat the sand grains, the irreducible water saturation of the formation increases, dramatically lowering the resistivity values. We assume that the grain consist of a non-conducting silicate core coated with a conductive clay. Lima and Sharma [5] proposed to employ the Hashin-Shtrikman upper bound for a coated sphere to obtain the effective electrical conductivity for the grains:

$$\sigma_s = \frac{\sigma_c \left[2p\sigma_c + (3-2p)\,\sigma_{sa}\right]}{(3-p)\,\sigma_c + p\sigma_{sa}} \tag{4}$$

where p is the volume fraction of the coating clay. For a non-conducting core ($\sigma_{sa} = 0$) as would be the case for most sandstone minerals, we have

$$\sigma_s = \frac{2p\sigma_c}{3-p} \tag{5}$$

This last equation can also be generalized to take into account different grain shapes [4]. As for Mixing-model 1 the effective conductivity of the whole rock is given by Eq. (2).

2.3. Mixing-model 3: Dispersed Clays

In this mixing-model the clay grains fill the pore space between sand grains. We will assume that the composite medium is built from an initial fixed volume of fluid by adding to it, in steps, infinitesimal amounts of insulating sand grains and clay aggregates. This procedure was proposed by Lima and Sharma [5] who adapted the incremental method first introduced by Feng and Sen [3]. The incremental method solution can be written as (assuming non-conducting core $\sigma_{sa} = 0$):

$$\sigma^* = \sigma_f \phi^{3/2} \left[\frac{1 + (1-3p)\,\sigma_c/2\sigma^*}{1 + (1-3p)\,\sigma_c/2\sigma_f}\right]^{3p/(1-3p)} \tag{6}$$

where p again is the volume fraction of clay in the solid portion. For the special case of $\sigma_f \gg \sigma_c$ Eq. (6) can be simplified to a Waxman-Smits type of equation [9], which also can be modified to handle the case of non-spherical grains.

2.4. Mixing-model 4: Laminar Shales

The last type is the *laminar-shale* model, which consist of sequences of shale layers between sand layers. The effect of thinly bedded sand-shale sequences on a macroscopic scale is electrical anisotropy. Hence, the effective conductivity parallel with the bedding will be different from the effective conductivity normal to the layers. The ratio between vertical and horizontal resistivity can be 2–10 for hydrocarbon reservoirs (up to 100 reported). For this mixing-model we first compute the effective conductivity of the sand and fluid system σ^*_{sand} employing Bussian/Hanai-Bruggeman theory. The effective conductivities (vertical and horizontal) of the laminar shale is now given by the Wiener bounds [10]:

$$\sigma^*_h = v_{\text{sand}}\sigma^*_{\text{sand}} + v_{\text{shale}}\sigma_{\text{shale}}\ , \quad \frac{1}{\sigma^*_v} = \frac{v_{\text{sand}}}{\sigma^*_{\text{sand}}} + \frac{v_{\text{shale}}}{\sigma_{\text{shale}}}\ , \quad v_{\text{sand}} + v_{\text{shale}} = 1 \tag{7}$$

where v_{sand} and v_{shale} are the volume fractions of sand and shale, respectively.

We now illustrate the basic functions of the modeling tool through an example of dispersed-clay type. Fig. 1(a) shows the calculation interface of this model option. The right part illustrates the basic physical principle of the modeling. The corresponding parameters can be input or loaded (by pressing the 'load' button) from an input file. The equivalent conductivity of the mixture can be calculated and displayed in a separate window. The calculation result together with the input parameters can be saved as an output file. Pressing the 'Analysis' button will open a new window (shown in Fig. 1(b)) where the sensitivity of the effective conductivity with respect to some key input parameters can be analyzed. The example in Fig. 1(b) shows the effect of varying the porosity.

3. EM-MODELING PROGRAM

We have developed a 1.5-D EM-modeling tool that calculates the EM response of four types of dipole sources in a layered medium: horizontal electrical dipole (HED), vertical electrical dipole (VED),

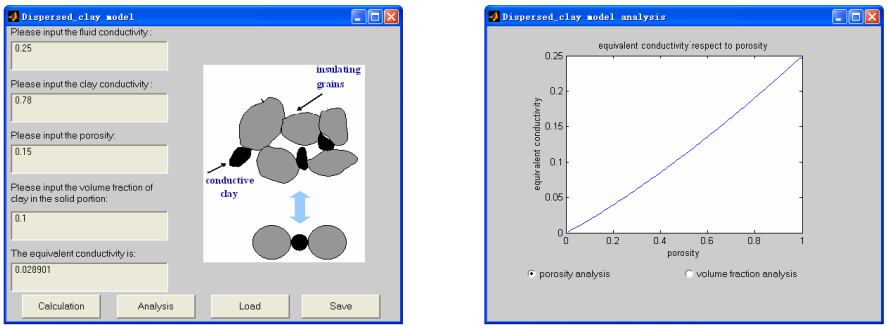

(a) (b)

Figure 1: Example of rock-physics modeling. (a) Calculation interface of dispersed clay model and (b) analyzing window showing the actual computations.

horizontal magnetic dipole (HMD) and vertical magnetic dipole (VMD). In SBL, the transmitter antenna is normally towed by a vessel at a depth just above the seabed. The receiver antenna (or eventually an array) is placed on the seafloor (in-line or cross-line polarized). The 1.5-D simulation software includes a graphical user interface and is based on J. A. Kong's formulations [6, 7]. In order to be as realistic as possible, the influence of the air layer in the limit of shallow water depths as well as the possibility of anisotropy caused by a finely layered reservoir (e.g., mixing-model 4) are also taken into account.

4. EXAMPLES OF THE INTEGRATED SYSTEM

In the following we limit our discussion to an isotropic case, hence mixing-models 1, 2 and 3. First, we employed our integrated modeling tool to study the variation in the EM response caused by the different clay distributions. The following parameters were used in the simulations: water conductivity: σ_w=*15.3846* S/m (with salinity of 100 kppm); effective porosity: ϕ=*0.15*; water saturation $S_w = 0.15$; conductivity of clay: $\sigma_c = 1.0$ S/m; saturation exponent: $n = 2$; volume fraction of clay in the solid portion: $p = 0.1$. The effective conductivity of the reservoir rock for the three different mixing-models were found to be: *structural clay* $\sigma^*_{\text{str.}}$=*0.1219* S/m; *coated clay* $\sigma^*_{coat..}$=*0.0903* S/m; *dispersed clay* $\sigma_{disp..}$=*0.0397* S/m.

Next, we established a 1-D layered-media model for the actual SBL simulations as showed in Table 1 below.

Table 1: The stratified media model for SBL

Layer	Thickness(m)	Conductivity(S/m)
Sea water	500	3.2
Layer1 overburden	1000	1
Layer2 reservoir	100	σ^* (coated, structural or dispersed clay)
Layer 3 half space	∞	1

In the simulations we assumed a fixed HED-source placed 50 meter above the seabed with an operating frequency of 0.25 Hz and 100 receivers deployed on the seabed (in-line direction and with a receiver interval of 100 m). Fig. 2 shows the magnitude of the E_ρ-*field* (i.e., the horizontal electric component along the in-line direction) normalized by the response from a homogenous subsurface for all three clay distributions. According to Fig. 2, all mixing-models are sensitive to the oil layer, but the dispersed clay model shows a much larger anomaly than the other two mixing model. The anomaly decreases as the offset increases (e.g., right half of the curves) due to strong airwaves. In the second experiment we considered the dispersed-clay model only and studied the effect of varying the brine salinity. Fig. 3 shows the normalized E_ρ-field of the HED source for three different salinity

values. The water conductivities corresponding to these salinity values are summarized in Table 2. From Fig. 3, it is evident that a high salinity corresponds to a large effective conductivity of the reservoir rock and consequently a low EM detectability.

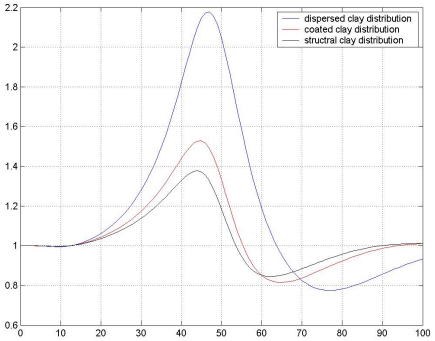

Figure 2: Normalized E_ρ-field for various clay models. Dispersed-clay (blue), coated-clay (red), structural-clay (black).

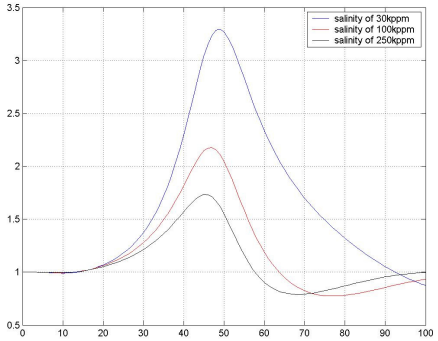

Figure 3: Normalized E_ρ-field for different salinities, (dispersed-clay model). 30 kppm (blue), 100 kppm (red) and 250 kppm (black).

Table 2: Variations in the effective conductivity of the reservoir rock and water conductivity due to different brine salinities.

Salinity(kppm) / Cond.(S/m)	30	100	250
σ_w	5.2632	15.3846	27.7778
σ^*	0.014979	0.039676	0.066

5. CONCLUDING REMARKS

From the examples above, it is evident that different clay distributions, keeping the volume fraction of clay constant, give rise to very different effective conductivities of the reservoir rock, and hence EM response. We have also seen that the salinity of brine in a sand-shale reservoir rock also affects the EM response considerably. In reality a hydrocarbon reservoir is more complex than the models discussed in this paper. However, we feel that the reservoir rock physics description introduced here will make EM-modeling more realistic offering useful information for further development of the SBL technique as well as for interpretation of SBL data.

ACKNOWLEDGMENT

We wish to thank the Norwegian Research Council, Hydro and Statoil for funding through a Petromaks project.

REFERENCES

1. Archie, G. E., "The electrical resistivity log as an aid in determining some reservoir characteristics," *Tran. AIME*, Vol. 146, 54–62, 1942.
2. Bussian, A. E., "Electrical conductance in a porous medium," *Geophysics*, Vol. 48, 1258–1268, 1983.
3. Feng, S. and P. N. Sen, "Geometrical model of conductive and dielectric properties of partially saturated rocks," *J. Appl. Phys.*, Vol. 58, 3236–3243, 1985.
4. Fricke, H., "A mathematical treatment of the electric conductivity and capacity of disperse system," *Phys. Rev.*, Vol. 24, 575–587, 1924.
5. Lima Olivar, A. L. and M. M. Sharma, "A grain conductivity approach to shaly sandstones," *Geophysics*, Vol. 55, 1347–356, 1990.

6. Kong, J. A., *Electromagnetic Wave Theory*, (ISBN 0-471-52214-7), 312–321, 1990.
7. Kong, J. A., "Electromagnetic fields due to dipole antennas over stratified anisotropic media," *Geophysics*, Vol. 37, 985–996, 1972.
8. Kong, F. N., H. Westerdahl, S. Ellingsrud, T. Eidesmo, and S. Johansen, "'Seabed logging': A possible direct hydrocarbon indicator for deepsea prospects using EM energy," *OIL & GAS Journal*, 2002.
9. Waxman, M. H. and L. J. M. Smits, "Electrical conductivities in oil-bearing shaly sands," *Soc. Petr. Eng. J.*, Vol. 8, 107–122, 1968.
10. Wiener, O., *Abh. Math. Phys. Kl. Sachs. Akad. Wiss.*, Lpz., Vol. 32, 509, 1912.

EAGE extended abstract:

Influence of Temperature on the Seabed Logging Response of a Sand-shale Reservoir

By

Wang, Z., Gelius, L.-J. and Kong, F.N.

69th EAGE Conference, London, 2007

Extended Abstract D044.

LONDON2007

D044

Influence of Temperature on the Seabed Logging Response for a Sand-Shale Reservoir

Z. Wang* (University of Oslo), L.J. Gelius (University of Oslo) & F.N. Kong (Norwegian Geotechnical Institute)

SUMMARY

Seabed logging (SBL) is a remote sensing EM technique with the potential of being a direct hydrocarbon indicator in marine environments. Temperature has a profound positive influence on both the conductivity of the pore fluid and the mobility of the counter-ions of clay in a water-saturated sand-shale reservoir. This paper first illustrates the influence of the temperature on the formation resistivity of different types of sand-shale reservoirs.Secondly, the change in the SBL EM-response caused by a steam-injection case associated with a simplified 1D reservoir model is presented. These simulation results clearly demonstrate that the increase of a reservoir temperature can imply a significant reduction in hydrocarbon detectability.

Introduction

Seabed logging (SBL) is a new remote sensing method employing EM energy to detect hydrocarbon bearing reservoirs offshore. The technique has been implemented commercially and has proved to give promising results (Kong et al. 2002, Farrelly et al. 2004). The key to this success is that electromagnetic waves are able to separate between oil and water as a pore fluid, based on their large differences in resistivity value.

The SBL method is currently being applied as a supplementary exploration method to seismic. Future use of the technique is foreseen to be within reservoir monitoring during production, employing permanent multi-component/multi-wave receiver arrays on the seafloor. In order to be able to carefully monitor the differences in the EM-response from such a producing reservoir over time, the resistivity changes caused by both variations in temperature and pressure (stress) must be accounted for. In this paper we will limit our discussions to the temperature effect and consider a sand-shale type of reservoir. Such a reservoir represents a very complex mixture including sand grains, clay particles, and pores filled with salt water and possible oil and /or gas. Hence, the effective resistivity of a sand-shale reservoir is affected by many parameters such as its geometric properties, content and salinity of salt water and content and distribution of clay (Feng and Sen, 1985). However, the formation resistivity is dominated by two parts: contribution from the salt water pore fill and contribution from the clay counter-ions. Both contributions are affected by the temperature. This paper first illustrates how the temperature affects the effective resistivity of a sand-shale reservoir in general. In addition, a simplified steam-injection case is included to demonstrate the importance of temperature on the final EM response.

A temperature dependent sand-shale reservoir model

We have adapted the earlier work of Sen and Goode (1992), who developed temperature dependent conductivity equations for shaly sands. In their model, the influence of temperature on both the conductivity of salt water and the clay counter-ions are considered. For partial saturated rocks their model reads as follows:

$$\sigma = S_w^n \phi^m \left(\sigma_w + \frac{1.93 m u_T Q_v}{1 + 0.7 u_T S_w^{-n} / \sigma_w}\right) + 1.3 u_T \phi^m Q_v \qquad (1)$$

$$u_T = 1 + 0.0414(T^oC - 22) \qquad (2)$$

and

$$\sigma_w = (5.6 + 0.27T - 1.5\,10^{-4}T^2)M - \frac{2.36 + 0.099T}{1.0 + 0.214\sqrt{M}} M^{3/2} \qquad (3)$$

where, the σ = formation conductivity; s_w = water saturation; n = saturation exponent; ϕ = porosity, m = cementation exponent; σ_w = water conductivity; T = temperature; u_T = mobility at a given temperature divided by that at room temperature; Q_v = clay counter-ion concentration per unit pore volume; M = molality of brine.

In the simulations we assumed a sand-shale reservoir with the following characteristics: ϕ = 15%, s_w = 15%, $m = n = 2$. We studied the resistivity of the sand-shale reservoir for different combinations of clay and NaCl brine:

(1) low water conductivity and low clay conductivity, e.g. M *=0.09 molal and* Q_v *=0.1 meq/ml.*

(2) high water conductivity and low clay conductivity, e.g. M *=4.74 molal and* Q_v *=0.1 meq/ml.*

(3) low water conductivity and high clay conductivity, e.g. M *=0.09 molal and* Q_v *=1.0 meq/ml .*

(4) high water conductivity and high clay conductivity, e.g. M *=4.74 molal and* Q_v *=1.0 meq/ml*

The formation resistivity (e.g. the reciprocal of the formation conductivity) corresponding to these four cases were now calculated employing Eqs. (1)-(3).

Table 1 and Fig. 1 show the computed results. Based on these findings we can draw the following conclusions:

- Contributions from both clay (Qv) and brine (M) to the formation resistivity are greatly affected by temperature.
- When water saturation is small (e.g. s_w=15%), clay counter-ions play a more important role than brine in the final contribution to the formation resistivity (compare the variation between the four lines in Fig.1).
- When both clay conductivity and brine conductivity are small, the formation resistivity has its largest dependence on the temperature (cf. green line in Fig.1). Whereas, when both clay conductivity and brine conductivity are large, the formation resistivity shows much smaller dependence on the temperature (cf. red line in Fig.1)

Table 1. Variations in specific resistivity ($r = 1/\sigma$ Ohm-m) with Qv, M and temperature.

Qv	M	22℃	50℃	80℃	110℃	140℃	170℃	200℃
0.1	0.09	294.5689	141.1604	90.7032	66.8747	52.9962	43.9121	37.5041
0.1	4.74	69.6800	39.4521	27.3996	21.2793	17.5936	15.1443	13.4100
1.0	0.09	33.5907	15.6230	9.9327	7.2815	5.7479	4.7482	4.0450
1.0	4.74	24.1472	11.9698	7.8122	5.8217	4.6545	3.8876	3.3454

The seabed logging response in case of steam injection

We have developed a 1.5D EM modeling software for seabed logging that can be easily linked to a rock-physics model. In order to study the influence of temperature on the seabed logging response, we made use of a simple 1D model representing a possible reservoir with an overburden (cf. Table 2).

Table 2. Simple 1-D reservoir model

	Thickness (m)	**Resistivity (Ohm-m)**
Sea water	4000	0.3125
Layer1 overburden	1000	1
Layer 2 reservoir	50	r (formation res. of reservoir)
Layer 3 half space	∞	1

Steam injection is a complex process as well documented by Butler and Knight (1998 and 1995) among others. In the simulations presented here we therefore introduce a rather simplified case. We assume an oil-bearing reservoir with the following initial characteristics: ϕ = 15%, s_w = 15% ($s_{gas} = 0$, $s_{oil} = 85\%$), $m = n = 2$, T = 20℃ M =4.74 molal and Q_v=1.0 meq/ml. It implies that the conductivities of both clay and pore fluid are quite high.

The formation or effective resistivity r of such a reservoir is 26.056 Ohm-m applying Eqs. (1)-(3). The corresponding EM response employing the seabed logging technique is given by the red dashed line in Fig. 2. After a period of steam injection we then assume that the oil saturation s_{oil} declines to 10%, gas saturation s_{gas} increases to 70% (gas originally dissolved in the oil is released due to the temperature rise), so the water saturation s_w now is 20% (these values are based on a case described by Zou, 2006). Because steam injection normally employs steam liquid with same salinity as the original pore fluid, we can assume that the salinity of the reservoir keeps constant with low steam injection rate. For simplicity, we assume a homogeneous steam flooding and that the temperature of the reservoir T increases from 20℃ to 200℃. The corresponding formation resistivity r is now 2.3857 Ohm-m. The EM response of the exploited reservoir employing the seabed logging technique is shown as the blue dashed curve in Fig. 2. Finally, the black solid curve in Fig. 2 is the SBL EM-response of a homogenous earth model without an oil reservoir.

In the above example, the most significant variation of the reservoir is represented by the change in temperature before and after exploitation. Fig. 2 shows that it is easy to detect the presence of the initial oil reservoir employing the seabed logging method. However, after exploitation employing steam injection the EM response is nearly identical with the response of that of a homogenous subsurface. Hence, wrong estimates of the remaining hydrocarbons still present can easily be obtained, if the effect of temperature variations is not taken properly into account. Actually, in this simple example there is still a large amount of gas present in the reservoir. Using this simplified production model, we easily see that the increased temperature can cause the reservoir to be almost transparent. In practice, the steam-injection will be a much more complex process and should be modelled using 2-D or 3-D programs. However, the main trend will still be valid, e.g. increased reservoir temperature will lower the detectability of possible hydrocarbons left. Hence, if the SBL method is employed during reservoir monitoring, corrections for possible temperature changes are vital.

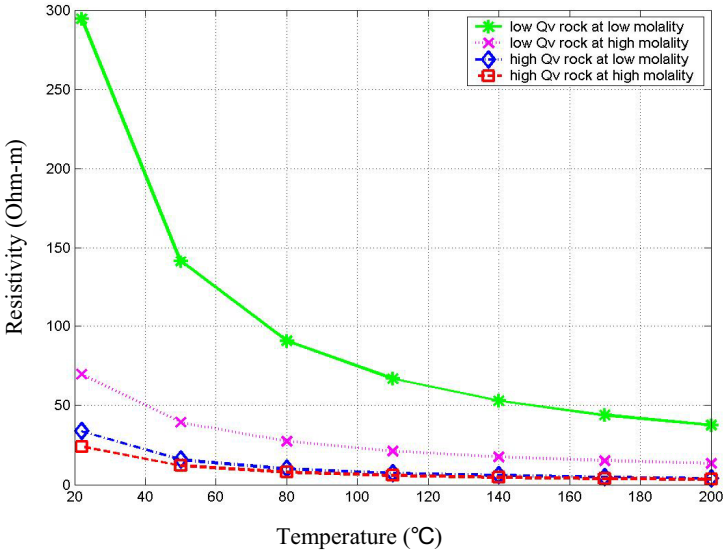

Figure 1. Variation of formation resistivitiy with respect to temperature.

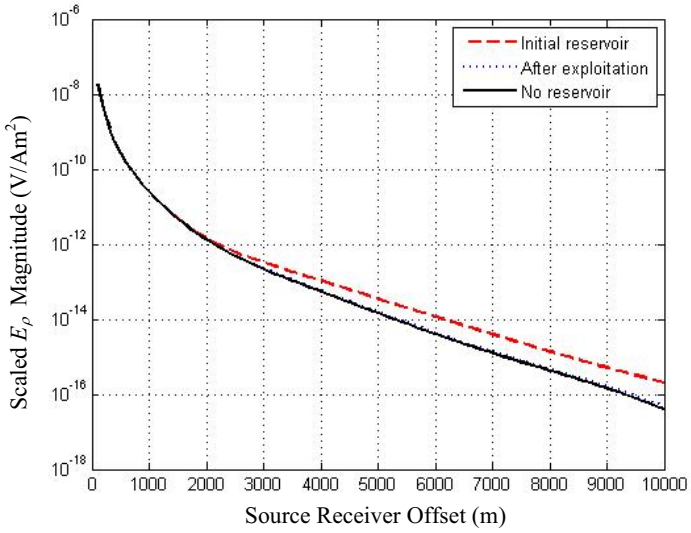

Figure 2. The EM responses of a petroleum reservoir. E_ρ is the horizontal electric component along the in-line direction excited by a unity horizontal electrical dipole source.

Conclusions

Temperature affects the formation conductivity of a sand-shale reservoir through two paths. Firstly, the temperature has a positive influence on the conductivity of the pore fluid. Secondly, the temperature has also a profound influence on the mobility of the counter-ions of clay, which is especially noticeable for a sand-shale reservoir with high clay content and low salinity. In reservoir monitoring employing seabed logging, the temperature is an important factor to be considered in the quantitative interpretation. As an example, in a steam injection case the increasing temperature will cause a lower hydrocarbon detectability.

Acknowledgements

We wish to thank the Norwegian Research Council, Hydro and Statoil for funding through a Petromaks project.

References

Butler David B., and Knight Rosemary J., [1998], Electrical conductivity of steam-flooded clay-bearing geologic materials, Geophysics, 63, 4, 1137-1149.

Butler David B., and Knight Rosemary J., [1995], The effect of steam quality on the electrical behaviour of steam-flooded sands: A laboratory study, Geophysics, 60, 4, 998-1006.

Farrelly B., Ringstad C. Johnstad S.E. and Ellingsrud S., [2004], Remote characterization of hydrocarbon filled reservoirs at the Troll Field by Sea Bed Logging, EAGE Fall Research Workshop on Advances in Seismic Acquisition Technology,Rhodes, Greece, September 19-23.

Feng, S., and Sen, P. N. [1985], Geometrical model of conductive and dielectric properties of partially saturated rocks: J. Appl. Phys., 58, 3236-3243.

Kong, F. N., Westerdahl, H. Ellingsrud, S, Eidesmo T. and Johansen S., [2002], 'Seabed logging': A possible direct hydrocarbon indicator for deepsea prospects using EM energy, Oil & Gas Journal, May 13, 30-38.

Sen P. N., and Goode P. A., [1992], Influence of temperature on electrical conductivity on shaly sands, Geophysics, 37, 89-96.

Zou Y. Bentley L. R., and Lines L.R., [2006], Integration of seismic methods with reservoir simulation ,Pikes Peak heavy-oil filed, Saskatchewan, The Leading Edge, 25, 6, 764-781.

SEG extended abstract:

A sensitivity analysis of the sea bed logging technique with respect to reservoir heterogeneities

By

Wang, Z., Gelius, L.-J. and Kong, F.N.

SEG Annual Meeting, Las Vegas, 2008, 711-715.

A sensitivity analysis of the sea bed logging technique with respect to reservoir heterogeneities

Zhong Wang and Leiv-J Gelius, University of Oslo; Norwegian Geotechnical Institute, Fan-Nian Kong, Norwegian Geotechnical Institute*

Summary

The sensitivity of a controlled-source EM (CSEM) method to various heterogeneities at reservoir level has been investigated. The simulation approach employed here is based on the combined use of a 2.5-D EM finite-element modeling program and a rock-physics simulator. Firstly, lateral variations in lithological parameters like porosity and shaliness were considered for a 2-D reservoir structure. In both cases the simulations indicated that the sensitivity of possible lateral gradients was poor when compared with the homogeneous average-value case. Hence, reservoir heterogeneities caused by lateral variations in lithology are not picked up easily by the CSEM technique due to its low-frequency limitation. However, in the second set of simulations the cause of the heterogeneities were due to variations in saturations in connection with a producing reservoir. Both the effect of secondary recovery represented by water flooding as well as EOR employing steam injection was simulated. The potential of the CSEM technique for such monitoring purposes was clearly demonstrated.

Introduction

The marine CSEM technique denoted Sea bed logging (SBL) (Eidesmo et al., 2002) has rapidly evolved as a complementary method to seismic when it comes to discrimination of pore fluid content. It is now applied routinely worldwide, but further knowledge of its limitations and areas of application is still in need. Forward modeling is an important tool both for survey planning and data interpretation as well as serving as an engine for inversion. However, standard modeling of SBL data utilize a simple and homogenous description of the potential hydrocarbon reservoir. This recognition has motivated the development of rock-physics based EM-modeling and a 1.5-D formulation has already been introduced and discussed by Wang et al. (2007a, 2007b). In this paper a more refined version of this modeling approach is introduced. A new rock-physics simulator based on a differential effective medium approach (Gelius and Wang, 2008) has been interfaced to a 2.5-D anisotropic finite-element EM-code (Kong et al., 2008). This combined tool is tailored for investigating the effect of various reservoir heterogeneities. Such inhomogeneities can be caused by distributions of temperature, pressure and saturation as well as spatial variations in lithology (shaliness, grain size distribution and alignment a.s.o.). Example of use of this modeling tool is demonstrated employing a layered test model and a 2-D hydrocarbon target. By introducing reservoir heterogeneities caused both by lithology and saturations, the sensitivity of the SBL technique can be studied carefully.

2-D test model employed in the sensitivity analysis

The test model is shown schematically in Fig.1, with the source being a horizontal electric dipole (HED) antenna with unit dipole moment and operating frequency of 1 Hz. It was placed 50m above the seafloor at the left boundary of the model. The water depth is 1000 m and its resistivity 0.3 Ohm-m. The model is gridded employing rectangular cells with dimension 100m x 50m. The hydrocarbon reservoir is 3000 m long and 150 m thick. Overlying the hydrocarbon layer, there is an anisotropic cap rock of shale characterized by a horizontal resistivity of 1 Ohm-m and a vertical resistivity of 2.5 Ohm-m (e.g. an anisotropy coefficient of 2.5).

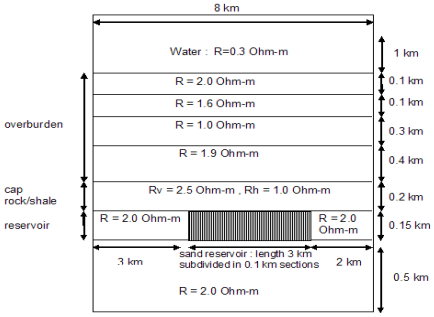

Figure 1: 2 D test model.

The reservoir zone consists of a total of 30 x 3 gridcells. Each cell is assigned a conductivity value employing the following rock-physics formulation (Gelius and Wang, 2008):

$$\sigma = \sigma_w (S_w \phi)^m \left(\frac{1 + l\sigma_c / \sigma}{1 + l\sigma_c / \sigma_w} \right)^n \qquad (1)$$

where σ is the effective conductivity; σ_w is the conductivity of brine; σ_c is the conductivity of possible clay; S_w is the water saturation; ϕ is porosity. l, m, n are parameters defining the shape and alignment of sand grains and possible clay aggregates.

Sensitivity to lithological parameters

In order to investigate the influence of porosity, a clean-sand reservoir target was assumed (spherical sand grains). The water saturation was set to 10% and the brine conductivity to 5 S/m. A collection of different porosity models were studied, each of them was representing a linear lateral gradient along the reservoir. Moreover, each model was chosen to have the same average porosity of 20%. The case of a uniform reservoir with 20% porosity was employed as the reference. By calculating the inline horizontal electric field along the seafloor, and for each model case normalizing the result by dividing it with the reference response, the curves in Fig.2 are obtained. For all cases considered, the sensitivity of the EM-response with respect to lateral variations in the porosity is found to be rather poor. Even for the largest gradient, the SBL technique gives an integrated response only a few percent different from the reference.

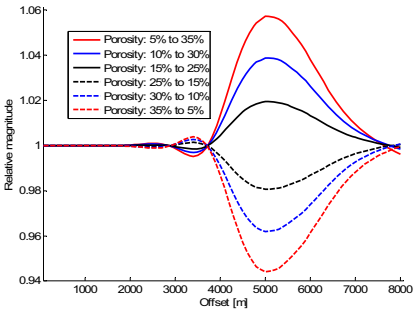

Figure 2. Plot of the normalized magnitude of the inline horizontal electric field for various linear-gradient porosity models (all having the same average of 20%). Reference case for normalization is a homogeneous reservoir with 20% porosity.

By analogy, the effect of lateral variations in shaliness was also investigated. This time the porosity was fixed to 30%, and the conductivity of brine and clay was set to 5 S/m and 0.5 S/m, respectively. In the simulations the water saturation was chosen to be 10%, whereas both the sand grains and the clay aggregates were assumed to be spherical. The reference case was a homogeneous clay content in the solid portion of 15%. Again, a family of different models were generated, each of them representing a linear clay variation across the target and with the same average value of 15% clay content. Plot of the normalized EM-responses (inline horizontal electric field component) for different clay-gradients are shown in Fig.3. Each of the responses was normalized by dividing them with the response from the uniform reference case. Once again is the sensitivity found to be low in general, and with each of the normalized curves showing a broad peak. From both Figs. 2 and 3 it can be seen that if the highest resistivity values are closest to the HED source it represents a positive normalized anomaly (and vice versa).

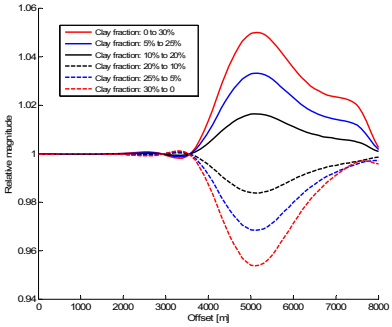

Figure 3. Plot of the normalized magnitude of the inline horizontal electric field for various linear-gradient shaliness models (all having the same average clay content of 15%). Reference case for normalization is a homogeneous reservoir with a 15% clay content in the solid portion.

The fairly poor sensitivity of the sea bed logging response to spatial variations of the lithology of the reservoir indicates clearly that an inversion of sea bed logging data should be constrained with additional information from seismic and possible log data.

Secondary recovery: water flooding simulation

Water is an effective fluid for maintaining reservoir pressure and driving oil towards a producer. Thus, it is the dominant secondary recovery technique. However, when the water saturation increases, oil is trapped as capillary forces cause the water to collect at pore throats. Thus, the water blocks movement of oil. Surfactants, polymers or foams reduce capillary forces and consequently the trapping of oil. In the simulations it is assumed such enhanced water flooding. Once more the 2-D model in Fig.1 is employed, and the sea bed logging response is calculated for different fluid front advances. The reservoir is assumed to consist of clean sand (mixture of spherical and disc type grains) with a porosity of 20% and its temperature is set to 50 °C. The salinity of the pore brine is assumed to be 30 kppm initially. Due to economic reasons, the flooding water is often used as produced water. Therefore, the salinity of injected water is also set here to 30 kppm. Before water flooding, the initial water saturation is 55% (homogeneous distribution) which is increased to 85% after the complete reservoir has been

flooded. Fig.4 shows the magnitude of the inline horizontal electric field component for various flood front advances. By introducing the initial phase before flooding as a reference, normalized responses can be computed as shown in Fig.5. In this example the injector was placed at that part of the target furthest away from the HED-source. Both figures show the decreasing EM response due to the replacement of hydrocarbons by injected salt water. Moreover, the slopes of these curves qualitatively describe the movement of the water flooding front. Hence, the sea bed logging technique seems rather sensitive to monitoring the fluid front advances compared to seismic.

Tertiary recovery: thermal or steam injection

For heavy or crude oil production, steam injection is widely applied to enhance oil recovery by heating the reservoir and consequently decreasing the viscosity of the crude oil. Again the 2-D simulation model from Fig.1 is employed, and by combining rock-physics and EM-modeling the corresponding sea bed logging response for consecutive steam flooding stages could be estimated.

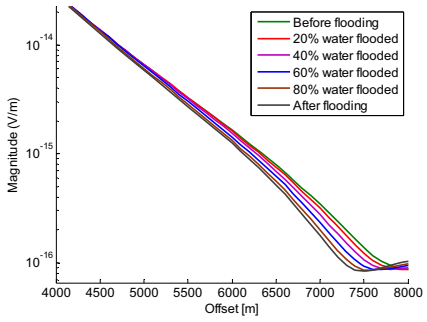

Figure 4. Magnitude of the inline horizontal electric field for various fluid front advances. (injector placed at the far end of target with respect to HED-source).

Steam flooding is a complicated process which gives rise to variations both in temperature, water saturation and salinity inside the reservoir. Butler and Knight (1995, 1998) studied the electrical behavior of steam-flooded sands with and without clay at laboratory scale. Moreover, they also developed a numerical model to simulate the high-quality steam flooding process. However, in their study, the targets were brine-saturated sands without any hydrocarbon fill. Based on their findings and extended to the hydrocarbon reservoir case, the simulations of the high-quality steam

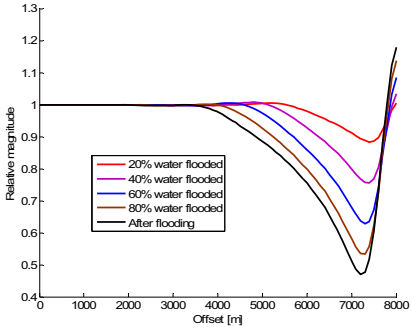

Figure 5. Normalized version of the responses in Fig.4, e.g. after dividing by the reference response (before flooding).

flooding process in a crude oil bearing target was carried out as follows. The initial conditions were taken to be: clean-sand reservoir at a temperature of 30 °C with spherical-type grains and a porosity of 20%. The brine saturation was 20% and the salinity was 30 kppm. Moreover, the steam quality was 80% which implies 80% of the feed water will be boiled into steam in the boiler (in the simulations the feed water as assumed to have the same salinity as the pore water). When the steam injection starts, the target can be split into four sections as shown in Fig. 6. The first section is the so-called steam-liquid section in which steam and liquid coexist and the liquid is mostly injected steam liquid. If one assumes a residual crude oil saturation of 30% after steam flooding, the saline liquid saturation in this area should be 14% (given a steam quality of 80%), with the remaining pore fill being steam or gas. The salinity of the liquid in this section is 150 kppm due to the evaporation of the feed water, and the temperature is assumed to raise to 180°C. The second part is the steam-condensation section which is integrated with the steam-liquid section to comprise the so-called steam zone. Within the steam-condensation section, the heated vapor which moves through the steam-liquid section condenses into distilled water. Thus, the liquid in this section is a mixture of condensed steam and original pore water and heavy oil. The water saturation will increase rapidly and the salinity decrease rapidly due to the condensation within this section. The temperature keeps the same as within the first section due to the heated vapor. Just ahead of the steam-condensation section is the mixed zone which is a fully liquid saturated region in which the condensed steam vapor mixes with and displaces original pore fluid. In this section, the temperature drops dramatically down to that of the undisturbed zone. The water saturation decreases and the salinity increases within this section also gradually to the values of the undisturbed zone.

The three plots in Fig.6 show the distribution of temperature, water saturation, salinity and resistivity along the target for three different steam front advances. As the steam injection evolves in time, both the steam zone and the mixed zone are expanded as shown in Fig.6. It can be easily seen that the transition of the resistivity from low to high value moves correspondingly with the steam front.
Fig. 7 shows the seabed logging responses at the seafloor for the three front advances shown in Fig.6 (magnitude of inline horizontal electric field component). In Fig.7 also the case of a completely flooded reservoir has been included. Fig.7 shows similar characteristics as Fig.4, but notice that the flood front now moves away from the source as opposed to the water-flooding example. The simulations clearly demonstrate the potential of a CSEM-type technique to monitor also the steam front advances (cf. the shift of the various responses).

Discussions

A combined 2.5-D modeling tool based on a rock-physics simulator interfaced to a finite-element EM-modeling code has been employed to test the sensitivity of the marine CSEM method to reservoir heterogeneities. The electromagnetic response resolves poorly lateral variations in lithology (porosity and shaliness) and should be combined with seismic for such purposes. However, in the case of reservoir monitoring in connection with EOR, the electric response is in general much more sensitive to saturation changes than the seismic method as expected.

Acknowledgments

The authors wish to thank the Norwegian Research Council and StatoilHydro for funding through a Petromaks project.

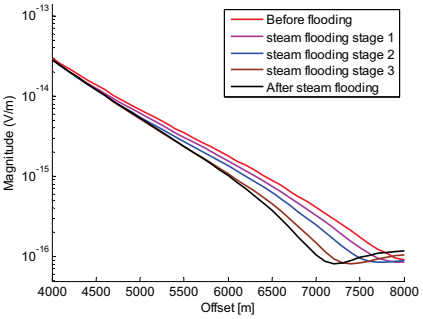

Figure 7. Magnitude of the inline horizontal electric field component for various steam front advances (injector placed at the closest end of target with respect to HED-source).

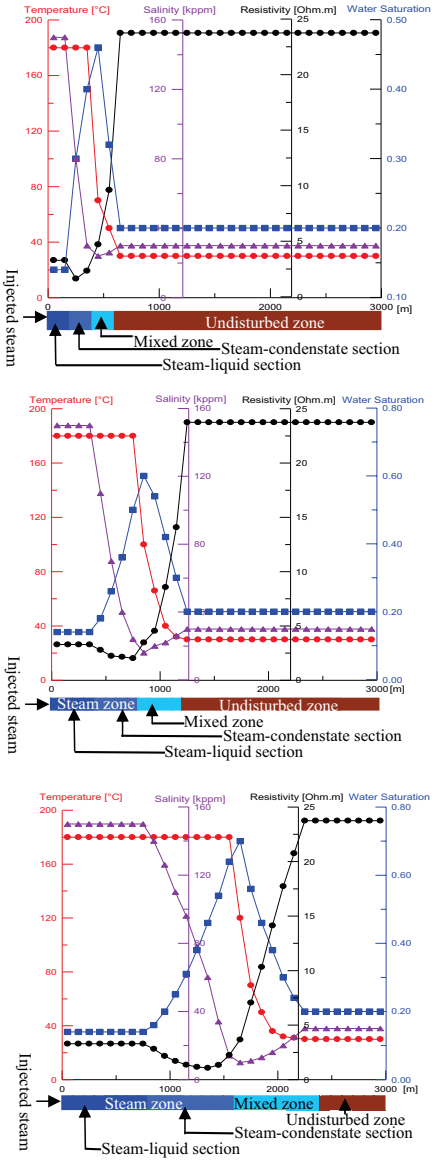

Figure 6. Three sequential stages of the steam flooding.

EDITED REFERENCES

Note: This reference list is a copy-edited version of the reference list submitted by the author. Reference lists for the 2008 SEG Technical Program Expanded Abstracts have been copy edited so that references provided with the online metadata for each paper will achieve a high degree of linking to cited sources that appear on the Web.

REFERENCES

Butler, D. B., and R. J. Knight, 1995, The effect of steam quality on the electrical behavior of steam-flooded sands: A laboratory study: Geophysics, **60**, 998–1006.

———1998, Electrical conductivity of steam-flooded, clay-bearing geologic materials: Geophysics, **63**, 1137–1149.

Eidesmo, T., S. Ellingsrud, L. M. MacGregor, S. Constable, M. C. Sinha, S. Johansen, F. N. Kong, and H. Westerdahl, 2002, Sea bed logging (SBL), a new method for remote and direct identification of hydrocarbon filled layers in deepwater areas: First Break, **20**, 144–152.

Kong, F. N., S. E. Johnstad, T. Røsten, and H. Westerdahl, 2008, A 2.5D finite-element-modeling difference method for marine CSEM modeling in stratified anisotropic media: Geophysics, **73**, F9–F19.

Gelius, L. J., and Z. Wang, 2008, Modeling production caused changes in conductivity for a siliciclastic reservoir: A differential effective medium (DEM) approach: Geophysical Prospecting (accepted).

Wang, Z., and L. J. Gelius, 2007a, Modeling of seabed logging data for a sand-shale reservoir: Progress in Electromagnetic Research Online, **3**, 236–240.

Wang, Z., L. J.Gelius, and F. N. Kong, 2007b, Influence of temperature on the seabed logging response of a sand-shale reservoir: 69th Annual International Conference and Exhibition, EAGE, Extended Abstracts, D044.

PIERS extended abstract (2):

Comparison of Antenna Types and Orientations for Detecting Hydrocarbon Layers in Seabed Logging

By

Johnstad, S.E., Westerdahl, H. Kong, F.N. and **Wang, Z.**

Progress in Electromagnetic Research Online, 2007

Vol. 3, No. 1, 52-55

Comparison of Antenna Types and Orientations for Detecting Hydrocarbon Layers in Seabed Logging

S. E. Johnstad[1], **H. Westerdahl**[2], **F. N. Kong**[2], **and Z. Wang**[2]

[1]Hydro Oil & Energy, Norway
[2]Norwegian Geotechnical Institute, Norway

Abstract— In seabed logging applications, only three types of sources: VED, HED-R (in-line) and HMD-P (cross line) are sensitive in detecting the target — a thin horizontal hydrocarbon layer. The other three types of the sources: VMD, HED-P (cross line), HMD-R are not sensitive in detecting the target.

DOI: 10.2529/PIERS060905055727

1. INTRODUCTION

For seabed logging measurements, there can be following basic types of sources: VED, VMD, HED and HMD. For horizontal antennas, there are two directions: in-line and cross-line. We use '-R' to represent in-line, and '-P' to represent cross-line. Hence there are six types of sources, i.e., VED, VMD, HED-R, HED-P, HMD-R, HMD-P. Obviously there are also six types of receiver antennas. Hence we have $6 * 6 = 36$ source/receiver combinations. In this paper we are going to investigate which source/receiver combinations are sensitive in detecting the thin hydrocarbon layers.

2. SENSITIVITY TO DETECT HYDROCARBON LAYER BASED ON GUIDE WAVE ASSUMPTION

We use the following table to show the sensitivity to detect hydrocarbon layer for different source/receiver combinations, where we use the words 'strong' and 'weak' to characterize the sensitivity in detecting the existence of a thin oil layer, and use 'zero' to mean no field is received for that combination.

Table 1: Sensitivity to detect hydrocarbon layer for different source/receiver combinations.

	Receiver VED	Receiver HED-R	Receiver HED-P	Receiver VMD	Receiver HMD-R	Receiver HMD-P
Source: VED	strong	strong	0	0	0	strong
Source: HED-R	strong	strong	0	0	0	strong
Source: HED-P	0	0	weak	weak	weak	0
Source: VMD	0	0	weak	weak	weak	0
Source:HMD-R	0	0	weak	weak	weak	0
Source:HMD-P	strong	strong	0	0	0	strong

The above table is based on our assumption that the main field components, which propagate inside a thin horizontal hydrocarbon layer, are the vertical E field and cross H field, referred to as the guide wave field components in [1]. Based on this assumption, the in-line HED and VED sources are considered being sensitive in detecting oil layers, since they can generate the guide wave fields inside the oil layer. The cross-line HED is not sensitive in detecting oil layers, since it can not generate the guide wave field components inside the oil layer.

The duality principle states that the fields generated by a magnetic source can be obtained from the fields generated by an electric source as long as following replacements are made:
$E \rightarrow H,\ H \rightarrow -E,\ \mu \rightarrow \varepsilon,\ \varepsilon \rightarrow \mu$. Hence HMD-R generates the fields as HED-P, and HMD-P generates the fields as HED-R. And VMD generates the fields that VED doesn't generate. We have then derived the results for the magnetic dipole sources shown in the table. In the next section we will use analytical results to verify the results shown in the table.

3. VERIFICATION BY ANALYTICAL RESULTS

The analytical solution for dipole antenna embedded in anisotropic layers (1D target) was developed by Wait [5] and J. A. Kong [2]. Wait's method uses the potential vector and J. A. Kong's method does not use the potential vector. Instead he uses the vertical E and H fields to represent the E and H fields in other directions. In our software implementation we have used J. A. Kong's method [2–4], which calculates all six field components for both electric and magnetic sources along any direction. Hence the software is suitable for verifying our comments on the comparison of antenna types and orientations for detecting hydrocarbon layers.

The model is shown in Figure 1, where the sea (0.3 ohm-m) depth is 2000 m, the target (an oil layer, 50 ohm-m) is at 1000 m below the seabed and 50 m thick, and the overburden has a resistivity of 1 ohm-m. The source is at 50 m above the seabed and the receiver array is placed on the seabed. Frequency 1 Hz is used for modeling.

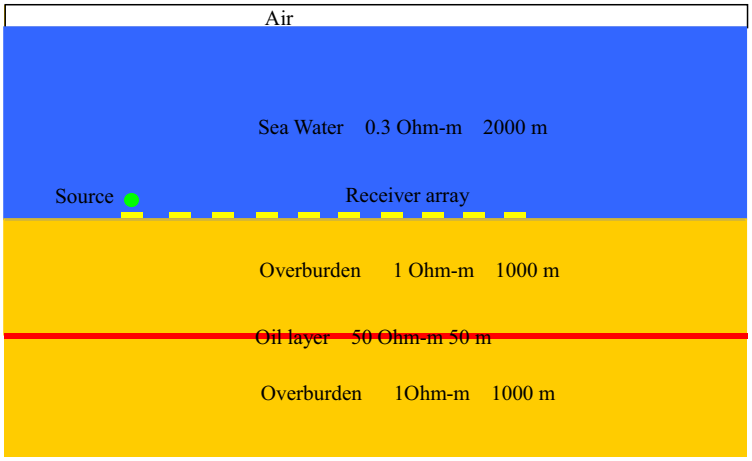

Figure 1: A seabed logging model.

Table 2: Corresponding figure numbers and curve colours for different source/receiver combinations.

	Receiver VED	Receiver HED-R	Receiver HED-P	Receiver VMD	Receiver HMD-R	Receiver HMD-P
Figure 6: Source, VED	(blue) strong	(red) strong	0	0	0	(green) strong
Figure 3: Source, HED-R	(blue) strong	(red) strong	0	0	0	(green) strong
Figure 2: Source: HED-P	0	0	(blue) weak	(red) weak	(green) weak	0
Figure 7: Source: VMD	0	0	(blue) weak	(red) weak	(green) weak	0
Figure 5: Source: HMD-R	0	0	(blue) weak	(red) weak	(green) weak	0
Figure 4: Source: HMD-P	(blue) strong	(red) strong	0	0	0	(green) strong

Figures 2–7 show the modeling results for different source types and orientations. To describe those figures, we have added the corresponding figure numbers and curve colors to Table 1, which leads to Table 2, for the modeling results for different source/receiver combinations.

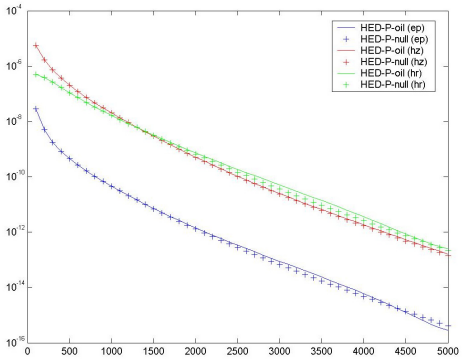

Figure 2: Received fields for HED source (cross). x-axis: receiver offset in meters.

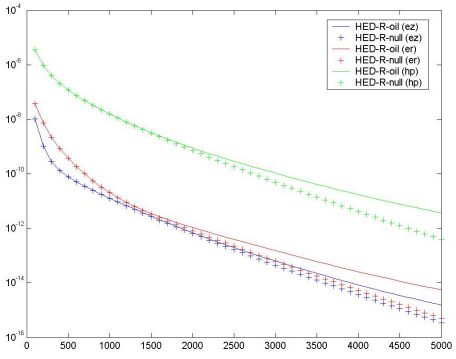

Figure 3: Received fields for HED source (in-line).

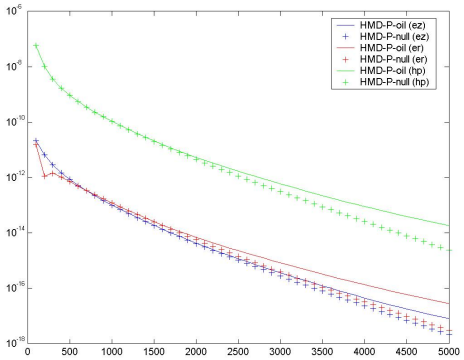

Figure 4: Received fields for HMD source (cross).

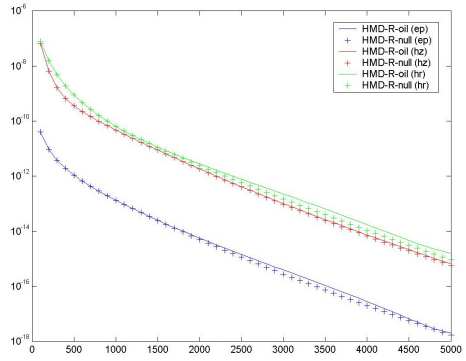

Figure 5: Received fields for HMD source (in-line).

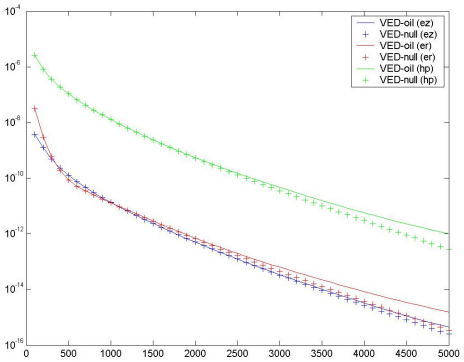

Figure 6: Received fields for VED source (cross).

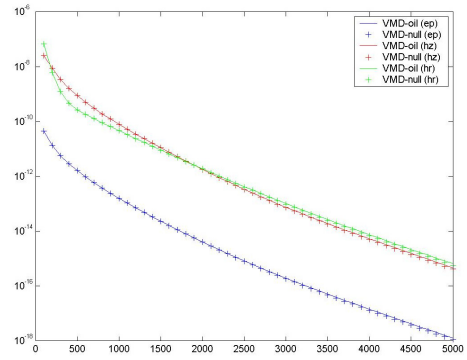

Figure 7: Received fields for VMD source.

In those figures, we use the dotted lines to show the fields received for the case without the oil layer, and use the solid lines to show the fields received for the case with the oil layer. When a field received with target has a larger difference to the field received without the target, we say this source/receiver combination has a strong response to the existence of the target. Otherwise we say the response is weak. From those figures we can see that our conclusion on the sensitivity of detecting a hydrocarbon layer shown in Table 1 is correct.

4. CONCLUSION

In seabed logging applications where a target is a thin horizontal hydrocarbon layer, The VED, HED-R (in-line) and HMD-P (cross line) are sensitive in detecting the target. The VMD, HED-P (cross line), HMD-R are not sensitive in detecting the target.

ACKNOWLEDGMENT

The authors wish to thank the Norwegian Research Council, Hydro Oil & Energy and Statoil for the finance support through a Peromaks project.

REFERENCES

1. Kong, F. N., H. Westerdahl, S. Ellingsrud, T. Eidesmo, and S. E. Johansen, "Seabed logging: A possible direct hydrocarbon indicator for deepsea prospects using EM energy," *Oil & Gas Journal*, May 13, 2002.
2. Kong, J. A., "Electromagnetic fields due to dipole antennas over stratified anisotropic media," *Geophysics*, Vol. 37, No. 6, 985–996, 1972.
3. Kong, J. A., *Electromagnetic Wave Theory*, Second Edition, John Wiley & Sons, Inc., 1990.
4. Tang, C. H., "Electromagnetic fields due to dipole antennas embedded in stratified anisotrpic media," *IEEE Trans. Antenna and Prop.*, Vol. AP-27, No. 5, Sep. 1979.
5. Wait, J. R., "Fields of a dipole over an homogeneous anisotropic half-space," *Can. Jour. Phys.*, Vol. 44, 2387–2401, 1966.